Available online at www.sciencedirect.com
ScienceDirect
International Journal of Pharmaceutics 342 (2007) 184–193
INTERNATIONAL JOURNAL OF PHARMACEUTICS
www.elsevier.com/locate/ijpharm

Pharmaceutical Nanotechnology

Photoregulation of drug release in azo-dextran nanogels

Satyakam Patnaik [a], Ashwani K. Sharma [a], B.S. Garg [b], R.P. Gandhi [c], K.C. Gupta [a,*]

[a] *Nucleic Acids Research Laboratory, Institute of Genomics and Integrative Biology, Mall Road, Delhi University Campus, Delhi 110007, India*
[b] *Department of Chemistry, University of Delhi, Delhi 110007, India*
[c] *Dr. B.R. Ambedkar Center for Biomedical Research, University of Delhi, Delhi 110007, India*

Received 5 March 2007; received in revised form 20 April 2007; accepted 20 April 2007
Available online 13 May 2007

Abstract

A simple photoresponsive azo-dextran polymer has been investigated for its ability to act as a nanogel drug carrier. Self aggregation of the azo-dextran polymer leads to the formation of nanogels, AD (**5** and **10**) in aqueous media, which were characterized by TEM and DLS. When examined under UV light (365 nm), the unloaded nanogels, which were observed to be in the range of 120–290 nm, show dependence on the degree of crosslinking, pH and ionic concentration of the dispersed media. Nanogels, AD (**5** and **10**), have been loaded with a model fluorophore, rhodamine B and a drug, aspirin, by freeze drying an aqueous dispersion of the nanogels in the presence of the substrate dissolved in water or PBS buffer. The release pattern of the encapsulated bio-active molecules from these nanogels was regulated by (*trans–cis*) photoisomerization of the azobenzene moiety present in the crosslinker. A comparison of the release behavior of the loaded (rhodamine, aspirin) AD (**5** and **10**) nanogels reveal that the rate of release of the encapsulated active molecules from the nanogels was slower when the azo moiety was in *E*-configuration as compared to that the azo in the *Z*-configuration. The in vitro release behavior of drug from these polymeric micellar systems is revelative of the potential of the nanogels for targeted drug delivery in nanomedicine.

Keywords: Photoisomerization; Nanogels; Drug delivery; Azo-dextran; Amphiphilic polymer

1. Introduction

The past few years have witnessed heightened interest in the development of new potent drugs in conjunction with site specific and controlled drug delivery systems. The latter studies have mainly focused on biopolymers, which are responsive to physiological changes such as pH, temperature and external stimuli such as light and, at the same time, can release an adaptable dosage of the therapeutic agent. In general, a photoresponsive water soluble polymer consists of a photoreceptor such as a photoisomerizable N=N moiety, and a hydrophilic polymeric backbone; the *trans–cis* photoisomerization in the chromophores results in a change in the physical (or chemical) properties such as morphology and degree of swelling of the biopolymers (Negishi et al., 1982; Maris et al., 2001; Yin et al., 2002; Ishihara et al., 1984). The above property of photoresponsive water soluble polymers makes them promising material for applications in drug delivery systems.

Amongst the photoresponsive groups, azobenzene functionality, in particular, has attracted special attention because of its ability to undergo reversible N=N *trans–cis* isomerization under UV–vis light as well as the fact that the azo moiety is cleavable by enzymes (azoreductases) produced by microflora of the gastrointestinal tract (Kakoulides et al., 1998; Kimura et al., 1992; Schacht et al., 1996; Ueda et al., 1996; Chung et al., 1992). Indeed, now there exists a large database citing azobenzene-induced effects on physical properties of a variety of polymers (Ikeda and Tsutsumi, 1995; Hu et al., 2002; Pieroni et al., 2001; Willner, 1997; Kumar and Neckers, 1989; Moss and Jiang, 1997; Anzai and Osa, 1994). Recently, various amphiphilic azobenzene-containing polymers self aggregate into micellar nanosize particles, which exhibit photoresponsive properties (Wang et al., 2004; Li et al., 2005; Ravi et al., 2005).

In the present work, we have developed photoresponsive self aggregated particles (nanogels), based on azobenzene and dextran [a neutral polysaccharide of 1,6-linked D-glucopyranose residues (Rotureau et al., 2004), which constitutes a potential

* Corresponding author. Tel.: +91 11 2766 2491; fax: +91 11 2766 7471.
E-mail address: kcgupta@igib.res.in (K.C. Gupta).

0378-5173/$ – see front matter © 2007 Elsevier B.V. All rights reserved.
doi:10.1016/j.ijpharm.2007.04.038

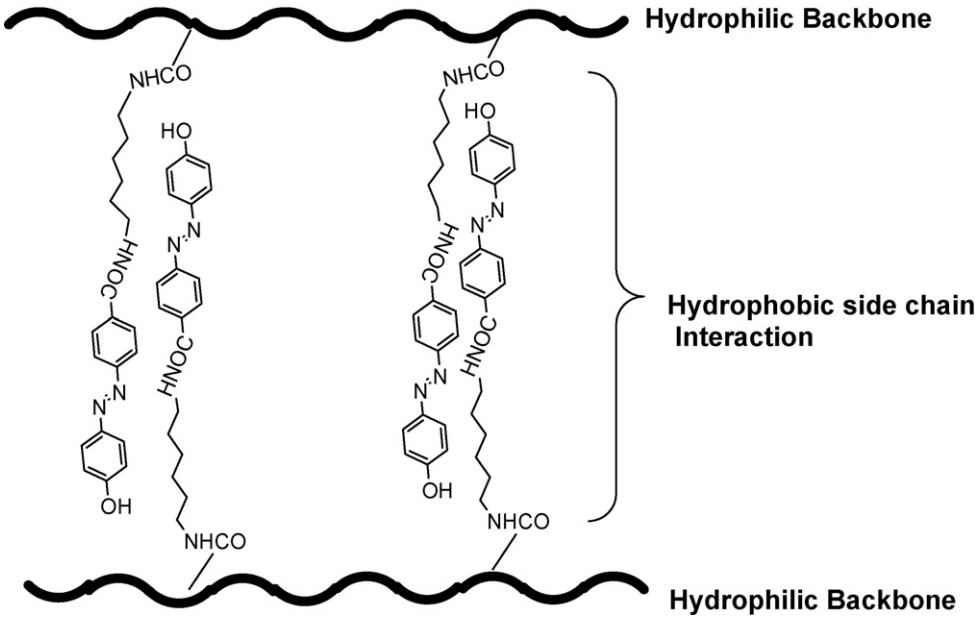

Scheme 1. Schematic representation of non-covalently crosslinked azo-dextran nanogels, AD (**5** and **10**).

system for drug delivery and controlled release of bioactive agents owing to its low cytotoxicity and high enzymatic degradation]. The paper reports rational design of a number of azobenzene grafted-dextran conjugates with varying degree of azo-to-polymer crosslink (mol%). In these, physical association of hydrophobic azobenzene side-chains in the (hydrophilic) backbone leads to emergence of micellar aggregates (nanogels), Scheme 1. On irradiation (*trans–cis*) isomerization of the azobenzene moiety in the cross-linked side chain results in weakening of hydrophobic interactions, and in matrix relaxation. The use of amphiphilic polymeric materials (to form nanogels) has the added advantage of facilitating drug permeation through biological membranes (Artusson et al., 1994; Aspden et al., 1996). Recently, several groups reported a variety of self assembled aggregates of amphiphilic polymers that have been used for various applications (Zhang and Eisenberg, 1995; Liu et al., 1996; Jenekhe and Chen, 1998; Massey et al., 1998; Won et al., 1999; Du and Chen, 2004). The paper further records observations on the above nanogels, when loaded with a model active molecule (rhodamine B, a dye) and a drug (aspirin), for determination of release patterns of the encapsulated active molecules under UV radiation.

2. Materials and methods

2.1. Materials

Dextran (M_w = 19,600), di-*tert*-butyl pyrocarbonate, hexane-1,6-diamine, Visking tube (M_w cut-off = 12–14 kDa), diisopropylcarbodiimide (DIPCI), *N*-(3-dimethylaminopropyl)-*N*′-ethylcarbodiimide hydrochloride (EDAC), eosin Y, *N*-hydroxysuccinimide (NHS), triethylamine (TEA), 3-(4,5-dimethylthiazol-2-yl)-2,5-diphenyltetrazolium bromide (MTT), Dulbecco's modified eagles media (DMEM) and deuterated solvents were purchased from Sigma–Aldrich, US. Cell culture products were purchased from Gibco-BRL-Life Technologies, Web Scientific Ltd., UK. Rhodamine B was purchased from Fluka. Thin layer chromatography was performed using silica gel $60F_{254}$; aluminium-backed plates (0.2 mm thickness) were purchased from E. Merck, Darmstadt, Germany. Column chromatography was carried out using silica gel (60–120 mesh size). Aspirin sodium salt was obtained (free sample) from SA Pharmacy, Sagar, India. Dimethyl formamide (DMF), dichloroethane (EDC) and dioxane are of analytical grade and are locally sourced. All solvents were dried and distilled prior to use.

2.2. Instrumentations

Mass spectra were recorded on a Hewlett-Packard 1100 MSD electron spray mass spectrophotometer in the linear negative mode. FTIR spectrum was recorded on a single beam Perkin-Elmer (Spectrum BX Series), with the following scan parameters: scan range 4400–400 cm^{-1}, number of scans 16, resolution 4.0 cm^{-1}. UV spectra were recorded on a Perkin-Elmer Lambda-Bio 20 UV–vis spectrophotometer. Fluorescence spectra were recorded on a Fluoromax-3, Jovin Yvon Horiba, Tokyo. TEM images were recorded on a Fei-Phillips, Morgagni 268D microscope. UV irradiation studies were performed in a photoreactor equipped with (10×15 W + 6×8 W = 198 W) UV lamps, from Gautam Enterprises, Delhi, India.

2.3. Synthesis

2.3.1. 4-(4′-Hydroxy-phenylazo)-benzoic acid 1

This was synthesized from 4-amino-benzoic acid (1.37 g, 10 mmol) and phenol (940 mg, 10 mmol) following the procedure given in the literature (Vogel, 1989). The pure product was obtained by chromatographic separation (silica gel; EDC,

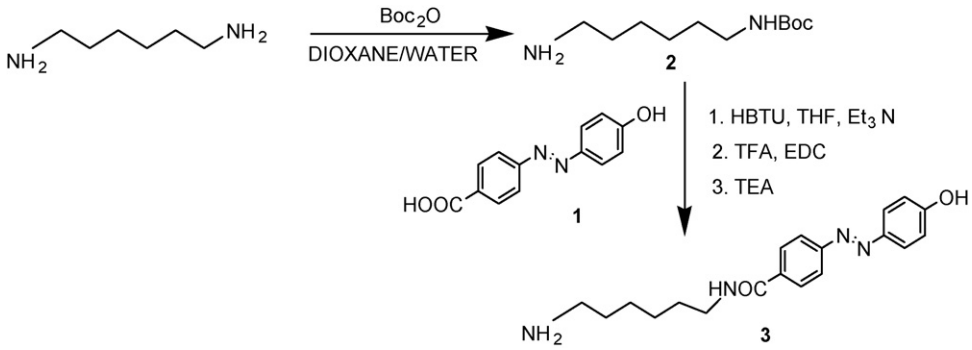

Scheme 2. Synthesis of linker, *N*-(6′-amino-hexyl)-4-(4″-hydroxy-phenylazo)-benzamide, **3**.

methanol), followed by recrystallization from ethanol. Yield: 740 mg (∼54%). IR: ν (cm^{-1}) = 1257, 1599, 1682, 2922, 3412. ^{1}H NMR ($CDCl_3$) δ: 8.25–8.27 (t, 2H, Ar–H), 7.9–7.95 (m, 2H, Ar–H), 6.9–7.05 (m, 4H, Ar–H), 4.54 (s, 1H, –OH).

2.3.2. *N-(6′-Amino-hexyl)-4-(4″-hydroxy-phenylazo)-benzamide 3*

Selective Boc-protection of hexane-1,6-diamine was achieved as shown in Scheme 2. To a solution of hexane-1,6-diamine (1.16 g, 10 mmol) in dioxane/water (1:1), di-*tert*-butyl pyrocarbonate (2.6 g, 1.2 mmol) was added dropwise, and the reaction mixture stirred overnight. After usual work-up, compound **2** was separated employing column chromatography using EDC/methanol eluent. Yield: 1.98 g (92%).

Coupling of the Boc-protected hexane-1,6-diamine, **2**, with **1** was achieved employing carbodiimide chemistry (Scheme 2). To a solution of **2** (215 mg, 1 mmol) and **1** (246 mg, 1 mmol) in THF was added NHS (154 mg, 1 mmol), followed by addition of coupling reagent, DIPCI (155 μl, 1 mmol). The reaction mixture was stirred overnight. After usual work-up, the product, Boc-*N*-(6′-amino-hexyl)-4-(4″-hydroxy-phenylazo)-benzamide, was isolated and purified through column chromatography technique (silicagel; EDC, methanol). Yield: 385 mg (∼88%). ^{1}H NMR ($CDCl_3$) δ: 8.27 (m, 2H, –NHCO–), 7.9–7.43 (m, 8H, Ar–H), 4.54 (s, 1H, –OH), 3.08 (m, 4H, $–CH_2–NH–$), 1.28–1.64 (m, 17H, –Boc and $–CH_2$). Boc deprotection of the above compound was achieved with TFA treatment, followed by removal of excess TFA and neutralization with TEA to give the desired product, **3**, in quantitative yield.

2.3.3. *Synthesis of azo-dextran polymers (AD **5** and **10**)*

Different degree (mol%) of carboxymethylation (CM) substitution on the dextran polymer were achieved as shown in Scheme 3; the percentage substitution was calculated using standard procedure (Zhang et al., 2005). In a typical experiment for achieving 10% carboxymethylation substitution on the dextran, 3.9 g dextran (20 kDa approx.) was dissolved in 50 ml of MQ water, followed by addition of 60 mg of sodium chloroacetate. Later, 10 ml of 8 M NaOH was added and the reaction mixture was diluted to 75 ml (MQ water); carboxymethylation was allowed to proceed for about an hour at 62 °C. The reaction mixture was quenched by lowering the solution's pH to 7 with 6 M HCl. The product was precipitated with 50 ml of absolute ethanol and allowed to stand overnight. The suspension was again redissolved in MQ water, followed by exhaustive dialysis in Visking tube (molecular cut-off = 12–14 kDa) for 72 h with water change at 6 h intervals. The dialyzed product was then freeze-dried to obtain a colorless fluffy material. The degree of substitution was ascertained by means of acid–base titration. The azo containing substrate, **3**, was then reacted with 10 mol% CM-dextran (Scheme 3). A 2 ml eppendrof was charged with a solution of CM-dextran (20 mg) in 1 ml water, followed by addition of *N*-hydroxysuccinimide (15 mg) and EDAC (20 mg). The resulting mixture was agitated slowly on a shaker. After about 3 h, a solution of **3** (5 mg) in DMF (500 μl) was added to the above CM-dextran mixture and slowly agitated on a shaker overnight. The solution was then dried in a speed vac, and the residue was redissolved in water, and washed with ethyl acetate. The aqueous layer was then dialyzed exhaustively in Visking tube (molecular cut-off = 12–14 kDa) for 72 h with water change at 6 h intervals. The dialyzed solution was then freeze-dried to give a light-yellow fluffy material. The modified azo-dextran (henceforth called AD nanogel) was characterized by IR: ν (cm^{-1}) = 1015–1156, 1275–1349, 1419–1457, 1590–1600, 1646, 2928 and 3400–3450. The presence of azo moiety in AD (**5** and **10**) nanogels was also confirmed by the changes in the UV spectral pattern at around 355 nm, when the polymeric samples were irradiated using UV light (Fig. 1).

2.4. *Photoisomerization of azo-dextran conjugates*

Photoisomerization of AD (**5** and **10**) nanogels in aqueous dispersion (2 mg/ml) was investigated using 365 nm radiation. The absorbance at 355 nm, which corresponds to the π–π* transition (*trans* azobenzene moiety), decreased with time, and the photostationary state was reached within 15 min of irradiation (Fig. 1). The dispersions were then kept in the dark and absorbance was recorded at different time intervals to determine the reversible isomerization process.

2.5. *Eosin quenching*

Eosin quenching experiments were performed to investigate the encapsulation active molecules in AD (**5** and **10**) nanogels and to examine conjugation of the azo derivative, **3**, with the

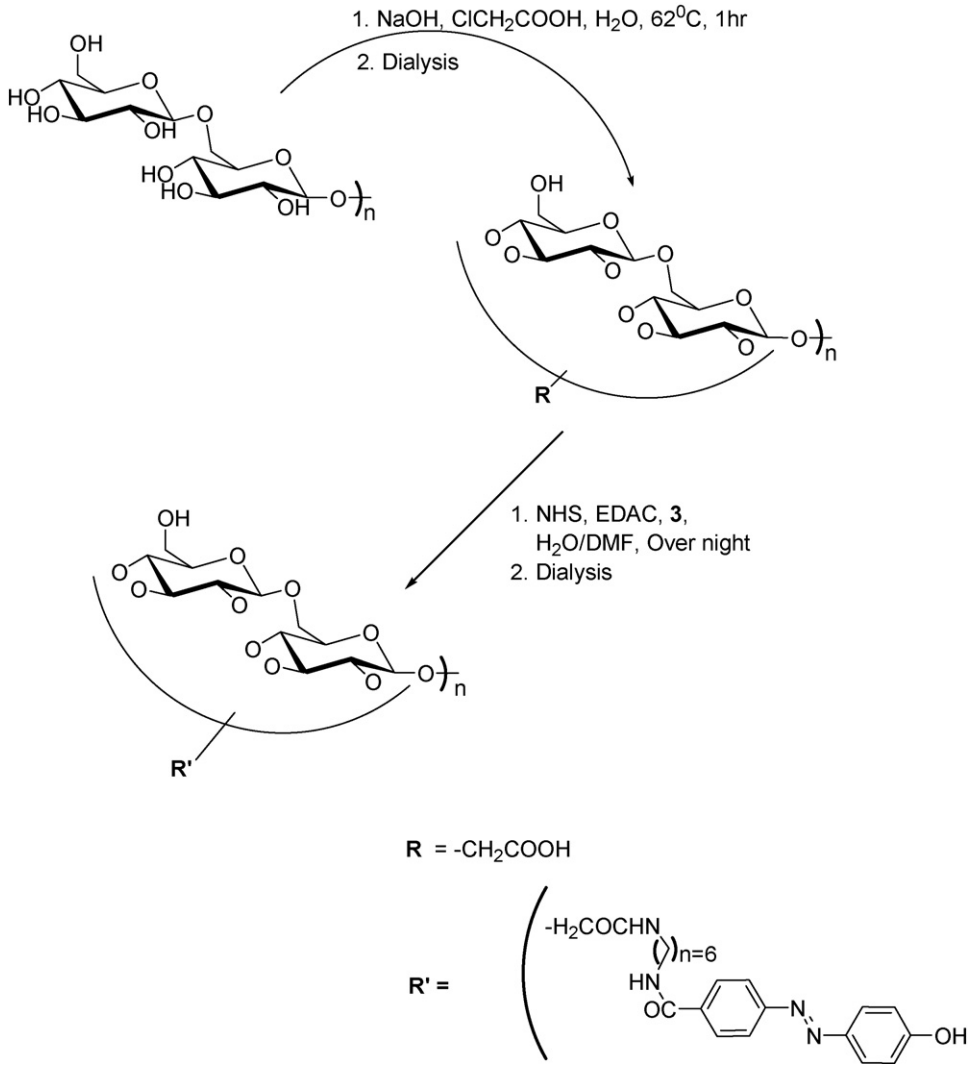

Scheme 3. Synthesis of photoresponsive azo-dextrans, AD (**5** and **10**).

dextran backbone. A 50 μl solution of (9.3×10^{-5} M) eosin Y was added to a 1 ml dispersion of AD (**5** and **10**) (3 mg/ml) each and fluorescence intensities (Exc. = 535 nm, Emi. = 570 nm) were recorded under the influence of UV and visible light.

2.6. Electron microscopy

Lyophilized samples (3 mg) of each loaded and unloaded AD (**5** and **10**), were dispersed in MiliQ water (1 ml), which was later

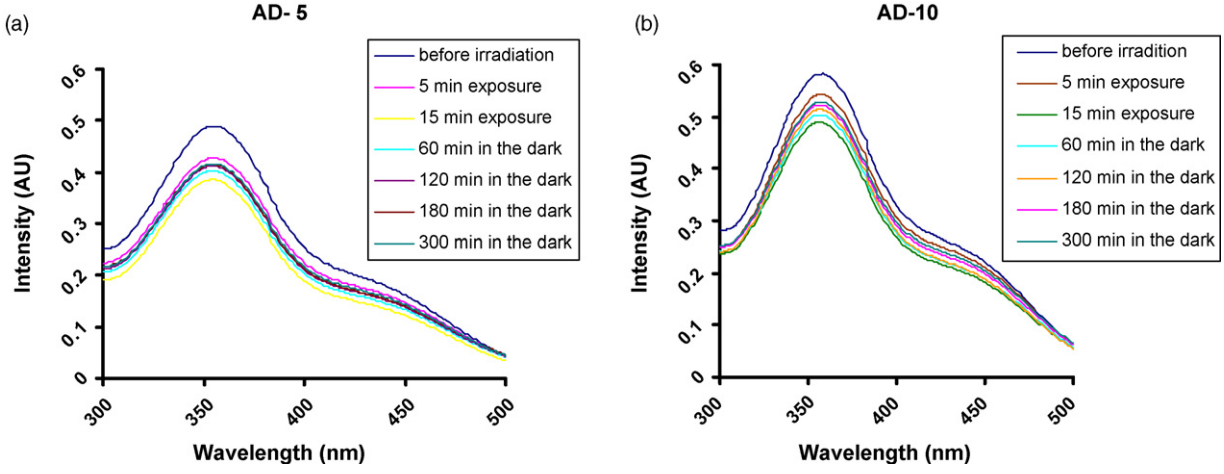

Fig. 1. Light-induced and thermal photoisomerization in azo-dextran nanogels, AD (**5** and **10**).

used for preparing samples for TEM. The sample dispersions (3 μl) were put on a formvar (polyvinyl formal) coated copper grid (200 mesh size) and air-dried. TEM pictures were taken on a Fei-Philips Morgagni 268D microscope. Prior to visualization of samples, the grids were negatively stained with saturated solution of uranyl acetate. Also scanned was a blank grid without the sample.

2.7. Gel deformation under irradiation

Gel deformation studies were carried out to examine the effect of UV radiation on the size of the nanogels in different buffer media. In a typical experiment, 4 mg of the freeze-dried samples of AD (**5/10**) were dispersed in 1.5 ml of desired buffer medium in an eppendrof. After vortexing, the hydrodynamic diameter of the modified nanogels was determined by dynamic light scattering (DLS) measurements before and after UV irradiation. Prior to size determination, all the dispersed media were filtered through 0.2 μm filters to remove dust particles. Nanogels size were determined using Zetasizer, Nano ZS (Malvern instruments, UK) employing a nominal 5 mW He–Ne laser operating at 633 nm wavelength at 25 °C. The scattered light was detected at 135° angle. Ultra pure water (refractive index, 1.33; viscosity, 0.89) was used for measurements at 25 °C. All data analysis was performed in automatic mode. Measured sizes represent the mean ± standard deviation of three independent experiments each having 20 runs.

2.8. Loading of rhodamine B in aqueous and buffer media

To a 5 ml aqueous dispersion of AD (**5/10**; 10 mg/ml), a solution of rhodamine B (0.05 mM, 250 μl) was added. The resulting mixture was irradiated with UV light inside the UV reactor (365 nm) for 1 h and then left overnight in the dark to facilitate the encapsulation process reversibly. The dispersion was then freeze-dried to give rhodamine B loaded AD (**5/10**) polymer as pink fluffy material. Similarly, rhodamine B loaded AD (**5** and **10**) polymers in different buffer media were obtained.

2.9. Loading of aspirin

To a 5 ml dispersed solution of AD (**5/10**; 25 mg in 2.5 ml of MQ water) was added 500 μl solution of aspirin sodium salt (10 mg/ml). The resulting mixture was then irradiated with UV light inside the UV reactor (365 nm) for 1 h and left overnight in the dark. The solution was then freeze-dried to give aspirin loaded AD (**5/10**) polymer as white fluffy material.

2.10. Release studies

In the release studies involving rhodamine B and aspirin loaded AD (**5** and **10**) (2 mg) nanogels, the polymers were dispersed, (a) in aqueous media (1 ml) and (b) in PBS (1 ml). The dispersed sample was then placed in 10 cm length of Visking tubing (molecular weight cut-off = 12–14 kDa) sealed at both ends and was dialyzed against aqueous/PBS (70 ml) in a set of two stoppered bottles. One of the bottles containing the nanogels was kept outside while the second one was placed inside the UV reactor, under irradiation (365 nm). One millilitre of the dialysate samples was taken from each of the bottles and was assayed for rhodamine B fluorimetrically (Exc. = 533 nm, Emi. = 614 nm) and for aspirin (λ_{max} = 296 nm) through UV measurements, at different time intervals. The data points represent the mean ± standard deviation of three independent experiments performed.

2.11. Biocompatibility assay

The toxicity of AD (**5** and **10**) nanogels was evaluated by MTT colorimetric assay (Mosmann, 1983). COS-1 cells were seeded onto 96-well plates at a density of 8×10^3 cells/well and incubated for 16 h for adherence. After 36 h, 50 μl MTT (3-(4,5-dimethylthiazol-2-yl)-2,5-diphenyltetrazolium bromide) (2 mg/ml in DMEM) was added to the cells and incubated for another 2 h. The MTT containing medium was aspirated, and the formazan crystals formed by the living cells were dissolved in 100 μl isopropanol containing 0.06 M HCl and 0.5% SDS. Aliquots were drawn from each well after 1 h of incubation and the absorbance measured spectrophotometrically in an ELISA plate reader at 540 nm. Untreated cells were taken as control with 100% viability, and cells without addition of MTT were used as blank to calibrate the spectrophotometer to zero absorbance. The relative cell viability (%) compared to control cells was calculated by $[abs]_{sample}/[abs]_{control} \times 100$.

3. Results and discussion

A spate of recent publications on drug release rate in polymers (Discher and Eisenberg, 2002; Haag, 2004; Hayashita et al., 1994; Munro et al., 1995; Kang et al., 2000; Lee and Mooney, 2001) reveals its dependence on the rate of swelling of the polymer network and on such properties of the external swelling medium as pH, ionic strength, buffer composition, temperature, and on factors such as hydrophobic–hydrophilic balance in the system and degree of crosslinking etc.(Groenewegen et al., 2000; Ravi et al., 2003; Zhang and Eisenberg, 1996; Lee et al., 2002; Tien et al., 2003).

In the present investigations, we have designed and synthesized some new water soluble photoresponsive azobenzene-crosslinked nanogels and studied the release patterns of model active molecules, rhodamine B and aspirin, when loaded onto the above nanogels.

3.1. Synthesis and characterization of azo-dextran polymers

The carboxymethylated dextrans were synthesized following the standard method (Zhang et al., 2005). Acid–base titration on the modified dextrans reveals the degree of carboxymethylation to be 9.4 ± 0.2% in case of 10% CM-dextran while 4.1 ± 0.3% was observed in the case of 5% CM-dextran. AD (**5** and **10**), with different molar ratio (mol%) of azo moieties to the polymer, were prepared by coupling of the carboxymethylated dextran with the

azobenzene linker, **3** (Scheme 3). The conjugation of the azo-linker, **3**, with dextran backbone was ascertained by IR and UV (vide experimental).

3.2. Photoisomerization of azo-dextran conjugates and eosin quenching studies

Photoisomerization of AD (**5** and **10**) nanogels dispersed in aqueous solution was investigated through irradiation at 365 nm. Fig. 1 shows maxima at 355 nm corresponding to π–π* transition (N=N trans), where the intensity is observed to decrease as the time of UV exposure increases. In both aqueous dispersion of nanogels of AD (**5** and **10**), photostationary state was reached within 15 min of irradiation (no further change takes place in the intensity of the band at 355 nm). The reversible *cis–trans* isomerization in the nanogels was studied in order to establish the stability of the *cis* form within the polymeric network, which is essential for sustained release of drugs. This was done by keeping the nanogels dispersion in the dark. It was observed that the reversible *cis–trans* isomerization process was relatively slow. The presence of the azo moiety and encapsulation of the active compound in the nanogels was established through eosin fluorescence quenching studies. It was observed that both the *E* and *Z* forms of the AD nanogels quench the eosin fluorescence. However, quenching by the *Z* isomers is more efficient than quenching by *E* isomer. The results thus obtained indicate that eosin is hosted within the nanogels (Fig. 2) (Archut et al., 1998).

3.3. Gel formation and deformation studies

Nanogels were formed by self aggregation of loaded and unloaded AD (**5** and **10**), in aqueous media. Fig. 3 (a and b) shows typical TEM micrographs of unloaded AD (**5** and **10**) nanogels (*trans*) while figures (c and d) show the same for (*trans*) loaded AD (**5** and **10**) nanogels. Gel deformation studies on AD (**5** and **10**) nanogels were carried out by DLS to determine the effect of UV radiation on the size of the nanogel in different buffer media. The results are summarized in Table 1. When examined under UV light (365 nm; Table 1), the size of the unloaded nanogels shows a dependence on the degree of crosslinking and pH of the dispersed medium. The average sizes of the loaded nanogels with entrapped molecules are revealed in Table 1. The observed decrease in size of the nanogels (with higher degree of crosslinking) is apparently due to greater propensity of the hydrophobic

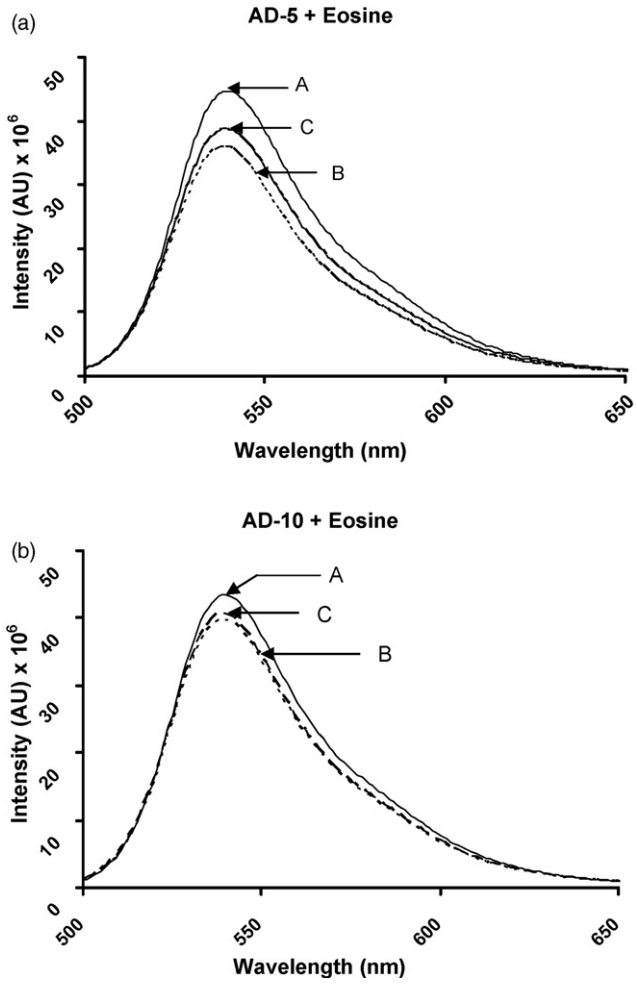

Fig. 2. Fluorescence measurements on azo-dextran nanogels, AD (**5** and **10**), curve A (—, line): solution containing eosin alone, curve B (– – –, line): solution containing both AD and eosin, when irradiated under UV light (365 nm) and C (- - -, line): solution containing both AD and eosin, when irradiated under visible light (>400 nm) (Exc. = 535 nm, Emi. = 570 nm).

moieties to form aggregates with compact cores in the polymeric network, as observed in AD **10** (when compared to AD **5**, which has a lesser degree of crosslinking). The increase in the average size of the nanogels due to *trans–cis* photoisomerization is reflective of weakened hydrophobic interactions, which results in loosening of the compact core in the matrix (Table 1). However, in case of the loaded nanogels, the results were consistent with the fact that a higher degree of crosslinking network enhances encapsulation (Xu et al., 2003) leading to formation

Table 1
Gel deformation measurements of unloaded and loaded (rhodamine B) azo-dextran nanogels, AD (**5** and **10**)

Nanogels	Average particle size (nm) determined by DLS ($n = 3$)					
	pH 4.0		pH 7.4		pH 9.0	
	trans	*cis*	*trans*	*cis*	*trans*	*cis*
AD 10 (unloaded)	125 ± 5	222 ± 6	177 ± 5	256 ± 2	204 ± 3	286 ± 4
AD 5 (unloaded)	182 ± 4	230 ± 3	210 ± 4	244 ± 8	238 ± 3	283 ± 5
AD 10 (rhodamine loaded)	204 ± 8	–	486 ± 9	–	620 ± 5	–
AD 5 (rhodamine loaded)	169 ± 3	–	280 ± 3	–	397 ± 4	–

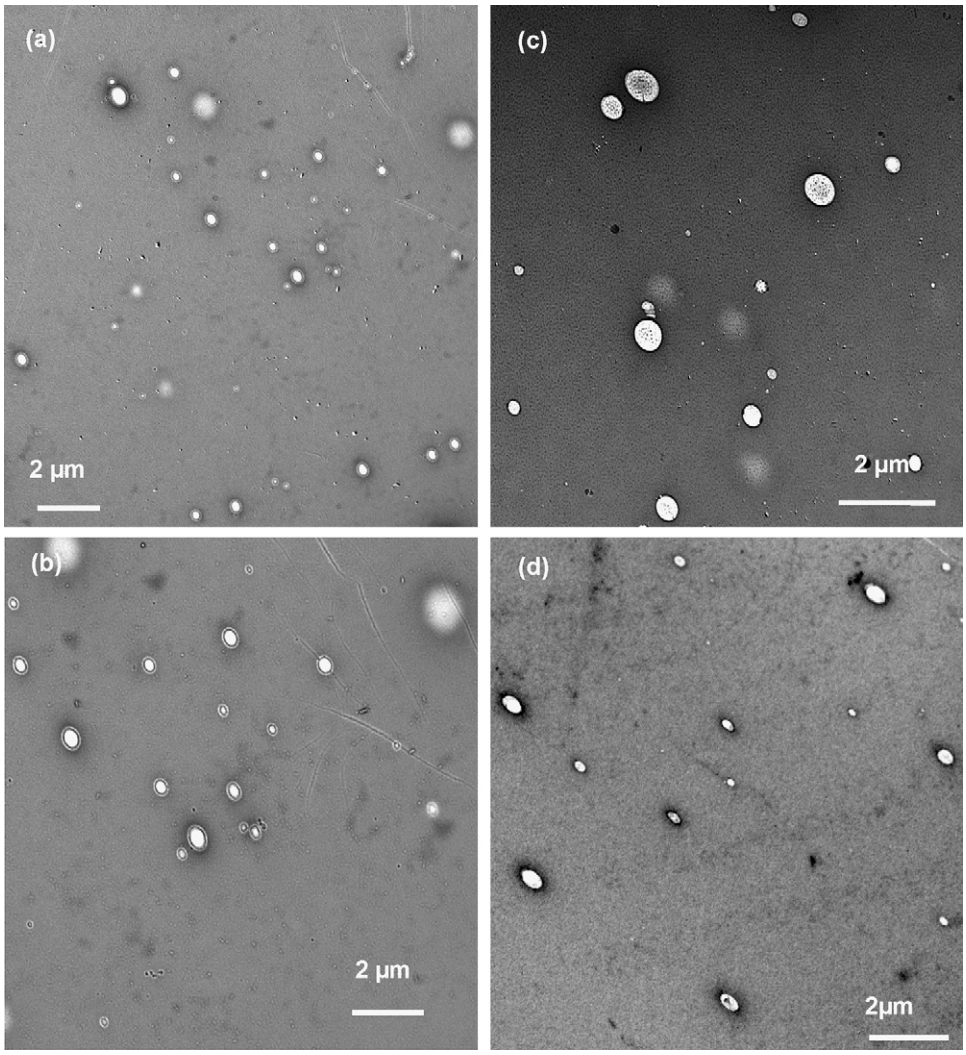

Fig. 3. TEM micrographs of nanogels prior to irradiation: (a, b) AD (**5** and **10**) unloaded and (c, d) AD (**5** and **10**) loaded with rhodamine B.

of bigger particles as seen through comparison of loaded AD **10** and AD **5**.

3.4. Biocompatibility assay

The cytotoxicity of AD (**5** and **10**) nanogels was assessed over the concentration range relevant to gene delivery by MTT assay. The level of toxicity was found to be a function of the degree of substitution and it decreased with increase in the azo substitution on dextran (Fig. 4). As is evident from the figure, the workable range for these AD nanogels is rather large i.e. from 1 to 300 (×10 μg/ml); above the concentration level of 300 (×10 μg/ml), nanogels become toxic to the cells.

3.5. Release studies

A comparison of the release behavior of various loaded (rhodamine, aspirin) AD (**5** and **10**) samples reveal that the rate of release of the encapsulated active molecules from the *E*-isomer of nanogels was slower as compared to that from the *Z*-isomer (Figs. 5 and 6). In this study, release pattern of the encapsulated molecules was evaluated using dialysis method in which the samples were dialyzed against aqueous/buffer (pH 4, 7.4 and 9, 0.1 M PBS buffer). The molecular weight cut-off (M_w cut-off = 12–14 kDa) of the semipermeable membrane employed allowed the drug/dye to be transported outside of the dialysis bag while retaining the nanogels within the dialysis bag. In each

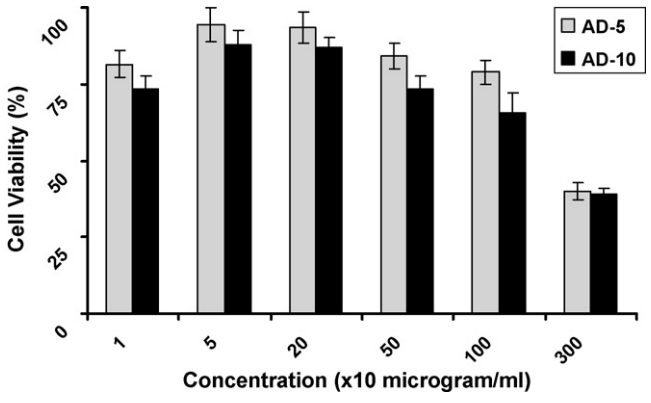

Fig. 4. Biocompatibility assay of azo-dextran nanogels, AD (**5** and **10**).

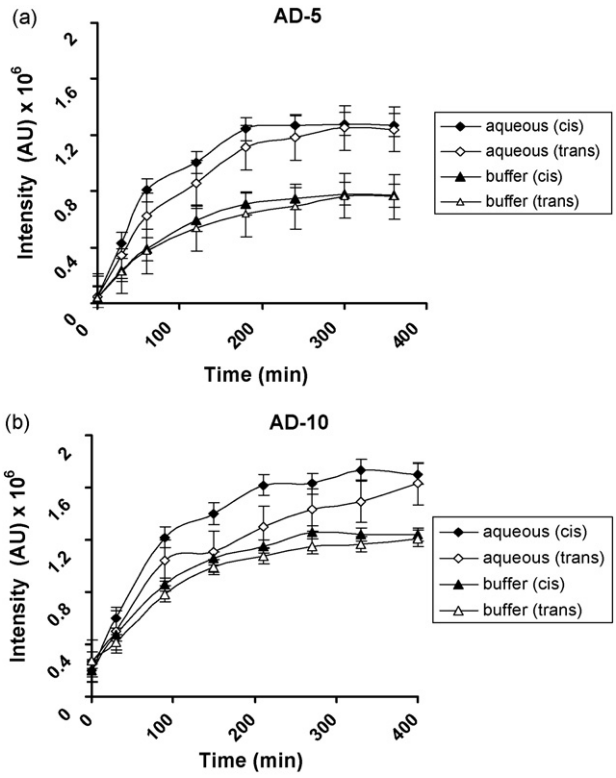

Fig. 5. Effect of dispersed media (aqueous and buffer, pH 7.4) on release pattern in azo-dextran nanogels, AD (**5** and **10**), during photoisomerization (Exc. = 535 nm, Emi. = 614 nm). *cis* (under irradiation, 365 nm), *trans* (in dark conditions).

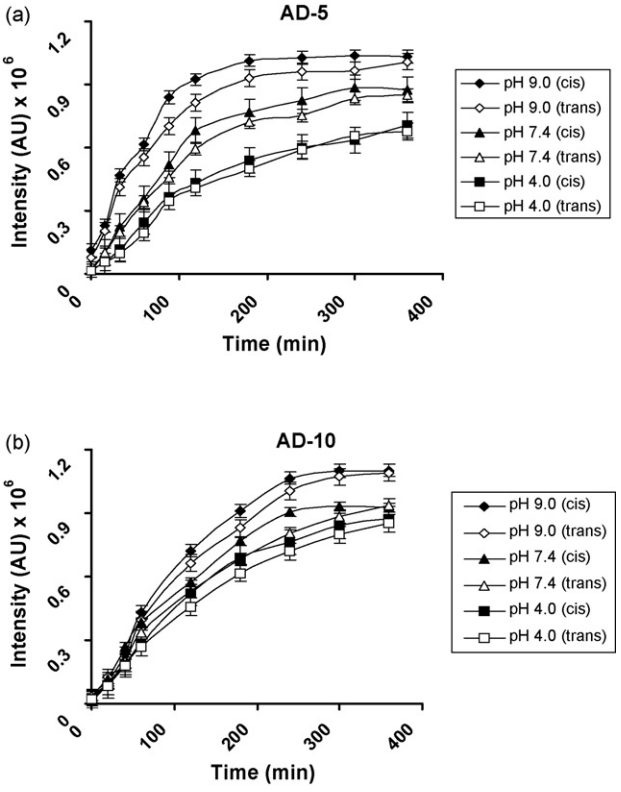

Fig. 6. Effect of pH on release pattern in azo-dextran nanogels, AD (**5** and **10**), during photoisomerization (Exc. = 535 nm, Emi. = 614 nm). *cis* (under irradiation, 365 nm), *trans* (in dark conditions).

set of experiments under UV and visible light, the experimental parameters were kept the same. Since the active molecule is physically entrapped in hydrophobic core of nanogels, it is speculated that the release of the active molecule from nanogels occurs mainly through diffusion. With the *trans–cis* isomerization in the nanogels, the hydrophobic interactions in cross-linked azobenzene side-chains (in nanogels) decrease with concurrent expansion (swelling) of the inner hydrophobic cavities, resulting in increase of diffusion rate of the drug through the polymer matrix.

We chose rhodamine B as a model substrate for studying the effect of dispersed media (salt and pH) on the release pattern during photoisomerization (Figs. 5 and 6, respectively). From a comparative release assay of the rhodamine molecule in aqueous and salt media (Fig. 5), it appears that, in aqueous media, a higher degree of swelling occurs loosening the hydrophobic interactions and the efficient isomerization in the azo moieties thus causes a faster release of the rhodamine molecule as compared to the nanogels dispersed in salt media. It is evident from Fig. 6 that there occurs an increase in release rate with increase in the pH of the dispersed medium. This is attributable to the fact that, at lower pH, the hydration of the nanogels diminishes, which causes swelling of the gel network to decline. The

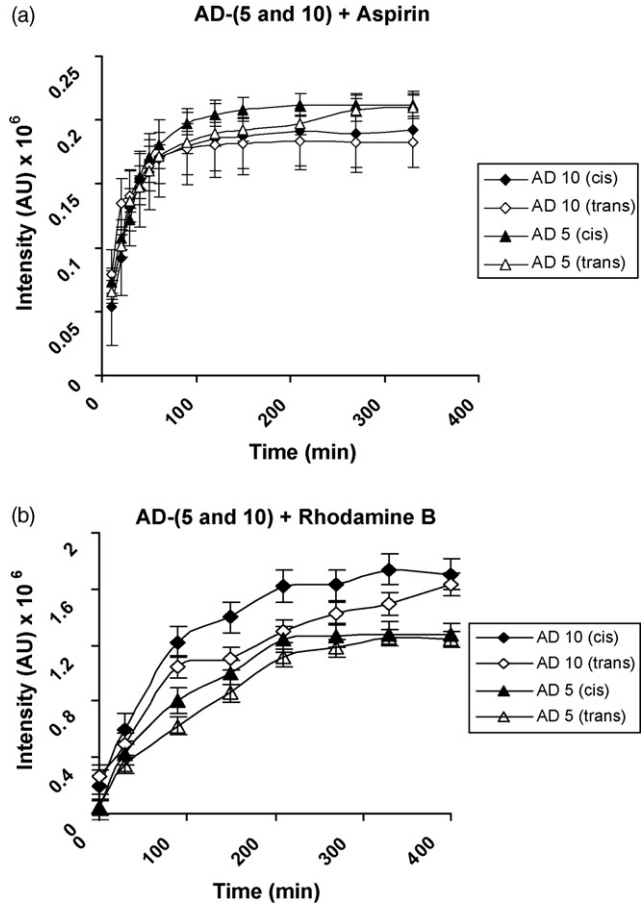

Fig. 7. Comparison of release pattern in aspirin- and rhodamine-loaded azo-dextran nanogels, AD (**5** and **10**) in aqueous media during photoisomerization (Exc. = 535 nm, Emi. = 614 nm). *cis* (under irradiation, 365 nm), *trans* (in dark conditions).

decrease in hydration of the gel network results in greater degree of interaction between various azo moieties thus restricting the degree of *trans–cis* photoisomerization upon irradiation. This further leads to slower rate of diffusion of the entrapped species from the gel matrix. However, at higher pH, the gels get effectively hydrated and swell adequately to cause a greater degree of *trans–cis* photoisomerization leading to faster rate of diffusion of the entrapped species from the hydrophobic pockets of the gel network.

However, a comparison of release pattern in aspirin and rhodamine loaded AD (**5** and **10**) nanogels in aqueous media (Fig. 7) reveals that while, in the former case, AD **5** nanogels permit the optimum controlled release, in the latter, the AD **10** nanogels display a higher release rate with respect to the AD **5** gels.

4. Conclusions

In this study, we report on a new class of photoresponsive nanogels based on non-covalently crosslinked azo-dextran nanogels for controlled release of drugs. It emerges that the *in vitro* release behavior of compounds from these polymeric micellar systems is influenced by their photoisomerization properties that in turn regulate hydrophobic characteristics of the nanogels. Again, the results indicate that the pH and salt concentration of the dispersed media affects the drug release rate involving the azo-dextran nanogels. These findings admit of potential therapeutic applications of nanogels systems in which controlled release of the drug molecule from the matrix is central towards the photoresponsive character of the linker moiety embedded in the polymer matrix.

Acknowledgements

Authors gratefully acknowledge financial support from Department of Biotechnology, New Delhi, India. TEM images were obtained at the sophisticated Analytical Instrumentation Facility (DST), AIIMS, New Delhi, India.

References

Anzai, J.I., Osa, T., 1994. Photosensitive artificial membranes based on azobenzene and spirobenzopyran derivatives. Tetrahedron 50, 4039–4070.

Archut, A., Azzellini, G., Balzani, C., Cola, V., De, L., Vogtle, F., 1998. Toward photoswitchable dendritic hosts. Interaction between azobenzene-functionalized dendrimers and eosin. J. Am. Chem. Soc. 120, 12187–12191.

Artusson, P., Lindmark, T., Davis, S.S., Illum, L., 1994. Effect of chitosan on the permeability of monolayers of intestinal epithelial cells (Caco-2). Pharm. Res. 11, 1358–1361.

Aspden, T.J., Illum, L., Skaugrud, Ø., 1996. Chitosan as a nasal delivery system: evaluation of insulin absorption enhancement and effect on nasal membrane integrity using rat models. Eur. J. Pharm. Sci. 4, 23–31.

Chung, K.T., Stevens Jr., S.E., Cerniglia, C.E., 1992. The reduction of azo dyes by the intestinal microflora. Crit. Rev. Microbiol. 18, 175–190.

Discher, D.E., Eisenberg, A., 2002. Polymer vesicles. Science 297, 967–973.

Du, J., Chen, Y., 2004. Preparation of organic/inorganic hybrid hollow particles based on gelation of polymer vesicles. Macromolecules 37, 5710–5716.

Groenewegen, W., Eigelhaaf, S.U., Lapp, A., van der Marrel, J.R.C., 2000. Neutron scattering estimates of the effect of charge on the micelle structure in aqueous polyelectrolyte diblock copolymer solutions. Macromolecules 33, 3283–3293.

Haag, R., 2004. Supramolecular drug-delivery systems based on polymeric core–shell architectures. Angew. Chem. Int. 43, 278–282.

Hayashita, T., Kurosawa, T., Miyata, T., Tanaka, K., Igawa, M., 1994. Effect of structural variation within cationic azo-surfactant upon photoresponsive function in aqueous solution. Colloid. Polym. Sci. 272, 1611–1619.

Hu, X., Zhao, X.Y., Gan, L.H., Xia, X.L., 2002. Synthesis, characterization, and photochromic properties of PMMA functionalized with 4,4″-diacryloyloxyazobenzene. J. Appl. Polym. Sci. 83, 1061–1068.

Ikeda, T., Tsutsumi, O., 1995. Optical switching and image storage by means of azobenzene liquid–crystal films. Science 268, 1873–1875.

Ishihara, K., Hamada, N., Kato, S., Shinohara, I., 1984. Photoinduced swelling control of amphiphilic azoaromatic polymer membrane. J. Polym. Sci. Polym. Chem. Ed. 22, 121–128.

Jenekhe, S.A., Chen, X.L., 1998. Self-assembled aggregates of rod-coil block copolymers and their solubilization and encapsulation of fullerenes. Science 279, 1903–1907.

Kakoulides, E.P., Smart, J.D., Tsibouklis, J., 1998. Azocrosslinked poly(acrylic acid) for colonic delivery and adhesion specificity: in vitro degradation and preliminary ex vivo bioadhesion studies. J. Control. Release 54, 95–109.

Kang, H.C., Min Lee, B., Yoon, J., Yoon, M., 2000. Synthesis and surface-active properties of new photosensitive surfactants containing the azobenzene group. J. Colloid. Interf. Sci. 231, 255–264.

Kimura, Y., Makita, Y., Kumagai, T., Yanane, H., Sasatani, T.K., Kim, S.I., 1992. Degradation of azo-containing polyurethane by the action of intestinal flora: its mechanism and application as a drug delivery system. Polymer 33, 5294–5299.

Kumar, G.S., Neckers, D.C., 1989. Photochemistry of azobenzene-containing polymers. Chem. Rev. 89, 1915–1925.

Lee, K.Y., Mooney, D.J., 2001. Hydrogels for tissue engineering. Chem. Rev. 101, 1869–1880.

Lee, A.S., Butun, V., Vamvakaki, M., Armes, S.P., Pople, J.A., Gast, A.P., 2002. Structure of pH-dependent block copolymer micelles: charge and ionic strength dependence. Macromolecules 35, 8540–8551.

Li, Y., He, Y., Tong, X., Wang, X., 2005. Photoinduced deformation of amphiphilic azo polymer colloidal spheres. J. Am. Chem. Soc. 127, 2402–2403.

Liu, G., Qiao, L., Guo, A., 1996. Diblock copolymer nanofibers. Macromolecules 29, 5508–5510.

Maris, B., Verheyden, L., Van Reeth, K., Samyn, C., Augustijns, P., Kinget, R., van den Mooter, G., 2001. Synthesis and characterisation of inulin-azo hydrogels designed for colon targeting. Int. J. Pharm. 213, 143–152.

Massey, J., Power, K.N., Manners, I., Winnik, M.A., 1998. Self-assembly of a novel organometallic–inorganic block copolymer in solution and the solid state: nonintrusive observation of novel wormlike poly(ferrocenyldimethylsilane)-*b*-poly(dimethylsiloxane) micelles. J. Am. Chem. Soc. 120, 9533–9540.

Mosmann, T., 1983. Rapid colorimetric assay for cellular growth and survival: application to proliferation and cytotoxicity assays. J. Immunol. Methods 65, 55–63.

Moss, R.A., Jiang, W., 1997. Thermal modulation of photoisomerization in double-azobenzene-chain liposomes. Langmuir 13, 4498–4501.

Munro, C.H., Smith, W.E., Armstrong, D.R., White, P.C., 1995. Assignments and mechanism of SERRS of the hydrazone form for the azo dye solvent Yellow 14. J. Phys. Chem. 99, 879–885.

Negishi, N., Ishihara, K., Shinohara, I., 1982. Complex formation of amphiphilic polymers with azo dyes and their photoviscosity behavior. J. Polym. Sci. Polym. Chem. 20, 1907–1916.

Pieroni, O., Fissi, A., Angellini, N., Lenci, F., 2001. Photoresponsive polypeptides. Acc. Chem. Res. 34, 9–17.

Ravi, P., Wang, C., Tam, K.C., Gan, L.H., 2003. Association behavior of poly(methacrylic acid)-block-poly(methyl methacrylate) in aqueous medium: potentiometric and laser light scattering studies. Macromolecules 36, 173–179.

Ravi, P., Sin, S.L., Gan, L.H., Gan, Y.Y., Tam, K.C., Xia, X.L., Hu, X., 2005. A comparison of the structure, thermal properties, and biodegradability of polycaprolactone/chitosan and acrylic acid grafted polycaprolactone/chitosan. Polymer 46, 137–146.

Rotureau, E., Leonard, M., Dellacherie, E., Durand, A., 2004. Amphiphilic derivatives of dextran: adsorption at air/water and oil/water interfaces. J. Colloid. Interf. Sci. 279, 68–77.

Schacht, E., Gevaert, A., Kenawy, E.R., Koen, M., Willy, V., Peter, A., Robert, C., Jan, G., 1996. Polymers for colon specific drug delivery. J. Control. Release 39, 327–338.

Tien, C.L., Lacroix, M., Ispas-Szabo, P., Mateescu, M., 2003. *N*-Acylated chitosan: hydrophobic matrices for controlled drug release. J. Control. Release 93, 1–13.

Ueda, T., Yamaoka, M., Miyamoto, M., 1996. Bacterial reduction of azo compounds as a model reaction for the degradation of azo-containing polyurethane by the action of intestinal flora. Bull. Chem. Soc. Jpn. 69, 1139–1142.

Vogel, A.I., 1989. Textbook of Practical Organic Chemistry, 5th ed. Longman Press.

Wang, G., Tong, X., Zhao, Y., 2004. Preparation of azobenzene-containing amphiphilic diblock copolymers for light-responsive micellar aggregates. Macromolecules 37, 8911–8917.

Willner, I., 1997. Photoswitchable biomaterials: en route to optobioelectronic systems. Acc. Chem. Res. 30, 347–356.

Won, Y.Y., Davis, H.T., Bates, F.S., 1999. Giant wormlike rubber micelles. Science 283, 960–963.

Xu, Y., Du, Y., Huang, R., Gao, L., 2003. Preparation and modification of *N*-(2-hydroxyl) propyl-3-trimethyl ammonium chitosan chloride nanoparticle as a protein carrier. Biomaterials 24, 5015–5022.

Yin, Y., Yang, Y., Xu, H., 2002. Hydrophobically modified hydrogels containing azoaromatic cross-links: swelling properties, degradation in vivo and application in drug delivery. Eur. Polym. J. 38, 2305–2311.

Zhang, L., Eisenberg, A., 1995. Multiple morphologies of "Crew-Cut" aggregates of polystyrene-*b*-poly(acrylic acid) block copolymers. Science 268, 1728–1731.

Zhang, L., Eisenberg, A., 1996. Morphogenic effect of added ions on crew-cut aggregates of polystyrene-b-poly(acrylic acid) block copolymers in solutions. Macromolecules 29, 8805–8815.

Zhang, R., Tang, M., Bowyer, A., Eisenthal, R., Hubble, J., 2005. A novel pH- and ionic-strength-sensitive carboxymethyl-dextran hydrogel. Biomaterials 26, 4677–4683.